

**ADSORPTION AND CORROSION INHIBITION OF SOME
POLYMERIC COMPOUNDS ON CARBON STEEL
IN ACIDIC SOLUTIONS**

A. M. Ouf^{a,b}, A.M. Abdelhafeez^a, H.A. Mostafa^a

^aDepartment of Chemistry, Faculty of Science, El-Mansoura
University, El-Mansoura-35516, Egypt.

^{a,b}Department of Chemistry, faculty of science and arts,
Taibah University , Al-Ula , Saudia Arabia

(Received: 7 / 8 / 2013)

ABSTRACT

The adsorption and corrosion inhibition effect of polymeric compounds the carbon steel in 0.5 M HCl solution was investigated by potentiodynamic polarization, electrochemical impedance spectroscopy (EIS) and electrochemical frequency modulation (EFM). The inhibitory property of the investigated compounds is discussed in terms of the mechanism by which its components adsorb onto the carbon steel surface. This adsorption process obeyed Langmuir adsorption isotherm. Investigated compounds act as a mixed-type inhibitor in 0.5 M HCl. The effect of the temperature on the corrosion rate was studied in the absence and presence of 300 ppm of polymeric compounds and the thermodynamic parameters of the corrosion process were calculated and discussed. The maximum inhibition approached 91.09% in the presence of 300 ppm polymeric compounds using electrochemical impedance spectroscopy technique. The results obtained from different electrochemical techniques were in good agreement.

Keywords: Carbon steel, Corrosion inhibition, Polymeric Compounds, HCl, Potentiodynamic polarization EIS, EFM.

1. INTRODUCTION

The use of inhibitors is one of the most practical methods to protect steel from corrosion, especially in acidic solutions where it is critical to prevent unexpected metal dissolution and acid consumption

(**Satapathy et al., 2009; da Rocha et al., 2010**). Most inhibitors used in industry are organic compounds primarily composed of nitrogen, oxygen and sulphur atoms. Inhibitors containing double or triple bonds play an important role in facilitating the adsorption of these compounds onto metal surfaces (**Torres et al., 2011**). A bond can be formed between the electron pair and/or the π -electron cloud of the donor atoms and the metal surface, thereby reducing corrosive attack in an acidic medium. Although many of these compounds have high inhibition efficiencies, several have undesirable side effects, even in very small concentrations, due to their toxicity to humans, deleterious environmental effects, and high-cost (**Parikh & Joshi, 2004**).

Polymers are attracting immense interest of researchers because of their good environmental stability, easy processability and easy modification of the electronic and optical properties by varying the synthesis parameters, suitable for application in different devices easily soluble in water (**Solomon et al., 2010**). Through their functional groups, they form complexes with metal ions and on the metal surface, these complexes occupy a large surface area there by blanketing the surface and protecting the metals from corrosive agents present in solution (**Rajendran et al., 2005**). The adsorbed film on metal provides barrier between metal and the medium. The objective of this study was to investigate the inhibitory effects of polymeric compounds as a corrosion inhibitor for carbon steel in 0.5 M hydrochloric acid by using weight loss, potentiodynamic polarization, electrochemical impedance spectroscopy and electrochemical frequency modulation.

2. EXPERIMENTAL

2.1. *Materials and solutions*

Experiments were performed using carbon steel of type 1018 with the following composition (weight %): C 0.2, Mn 0.35, P 0.24, Si 0.003 and balance Fe. The aggressive solution used was prepared by dilution of analytical Analar grade HCl (BDH) with bi-distilled water. The stock solution (500 ppm) of polymeric compounds (BDH) was used to prepare the desired concentrations by dilution with bi-distilled water. The concentration range of polymeric compounds used was (10 - 300 ppm).

2.2. Preparation of polymeric solutions

250 ml stock of the polymeric compounds were prepared by dissolving an accurately weighed quantity (0.125 gm) of each material in the appropriate volume of bi-distilled water. Appreciate concentrations (10 - 300 ppm) were prepared by dilution with bi-distilled water.

2.3. Weight loss method

The C-steel specimens used were cut from carbon steel sheet having surface area 2 x 2 x 0.2 cm. Before measurements were undertaken, the samples were abraded with emery paper 80, 220, 400, 600, 1000 and 1200 grades, degreased in acetone, rinsed with bi-distilled water and finally dried between two filter papers and weighed.

$$\Delta W = (w_1 - w_2)/a \quad (1)$$

Where w_1 and w_2 are the weights of the specimen before and after reaction, respectively, and (a) is the surface area in cm^2 .

Then the tests were prepared at different temperatures. The inhibition efficiency (η) and the degree of surface coverage (θ) of investigated inhibitors on the corrosion of carbon steel were calculated as follows:

$$\eta \% = \theta \times 100 = [(W_o - W)/W_o] \times 100 \quad (2)$$

Where W_o and W are the values of the average weight loss without and with addition of the inhibitor, respectively.

2.4. Electrochemical measurements

Electrochemical experiments were performed using a typical three-compartment glass cell consisted of the carbon steel specimen as working electrode (1 cm^2), saturated calomel electrode (SCE) as a reference electrode and a platinum wire (0.5 cm^2) as a counter electrode. The reference electrode was connected to a Luggin capillary and the tip of the Luggin capillary is made very close to the surface of the working electrode to minimize IR drop. All the measurements were done in solutions open to atmosphere under unstirred conditions. All potential values were reported versus SCE. Prior to every experiment, the electrode was abraded with successive different grades of emery paper, degreased with acetone, washed with bi-distilled water, and finally dried. Tafel polarization curves were obtained by changing the electrode potential automatically from (-500 to 500 mV vs. SCE) at open circuit potential with a scan rate of 2 mVs^{-1} . Stern-Geary method (**Parr et al.**,

1978) used for the determination of corrosion current is performed by extrapolation of anodic and cathodic Tafel lines to a point which gives $\log i_{\text{corr}}$ and the corresponding corrosion potential (E_{corr}) for inhibitor free acid and for each concentration of inhibitor. Then i_{corr} was used for calculation of inhibition efficiency (η %) and surface coverage (θ) as in equation 3:

$$\eta \% = \theta \times 100 = [1 - (i_{\text{corr(inh)}} / i_{\text{corr(free)}})] \times 100 \quad (3)$$

where $i_{\text{corr(free)}}$ and $i_{\text{corr(inh)}}$ are the corrosion current densities in the absence and presence of inhibitor, respectively.

Impedance measurements were carried out in frequency range from 100 kHz to 0.1 Hz with amplitude of 5 mV peak-to-peak using ac signals at open circuit potential. The experimental impedance was analyzed and interpreted based on the equivalent circuit. The main parameters deduced from the analysis of Nyquist diagram are the charge transfer resistance R_{ct} (diameter of high-frequency loop) and the double layer capacity C_{dl} . The inhibition efficiencies and the surface coverage (θ) obtained from the impedance measurements are calculated from equation 4:

$$\eta \% = \theta \times 100 = [1 - (R_{\text{ct}}^{\circ} / R_{\text{ct}})] \times 100 \quad (4)$$

where R_{ct}° and R_{ct} are the charge transfer resistance in the absence and presence of inhibitor, respectively.

Electrochemical frequency modulation, EFM, was carried out using two frequencies 2 and 5 Hz. The base frequency was 0.1 Hz, so the waveform repeats after 1 s. The higher frequency must be at least two times the lower one. The higher frequency must also be sufficiently slow that the charging of the double layer does not contribute to the current response. Often, 10 Hz is a reasonable limit. The Intermodulation spectra contain current responses assigned for harmonical and intermodulation current peaks. The larger peaks were used to calculate the corrosion current density (i_{corr}), the Tafel slopes (β_{c} and β_{a}) and the causality factors CF-2& CF-3 (Abdel-Rehim et al., 2006; Bosch et al., 2001). The electrode potential was allowed to stabilize 30 min before starting the measurements. All the experiments were conducted at $30 \pm 1^{\circ}\text{C}$.

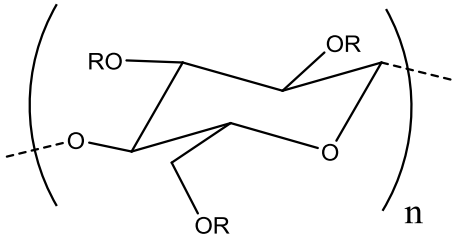
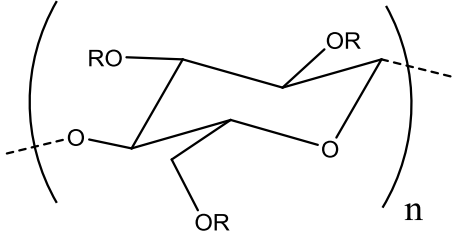
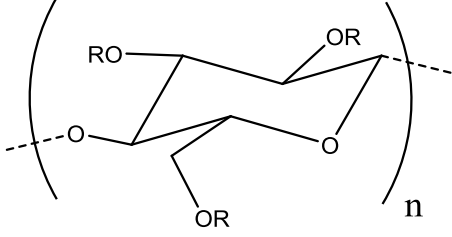
All electrochemical measurements were performed using Gamry Instrument (PCI4/G750) Potentiostat/Galvanostat/ZRA. This includes a Gamry framework system based on the ESA 400. Gamry applications

include DC105 software for potentiodynamic polarization measurements, EIS300 software for electrochemical impedance spectroscopy and EFM 140 software for electrochemical frequency modulation measurements along with a computer for collecting data. Echem Analyst 6.03 software was used for plotting, graphing, and fitting data.

To test the reliability and reproducibility of the measurements, duplicate experiments were performed in each case at the same conditions.

The polymeric compounds used in this study are listed in Table 1.

Table (1): Chemical structures of inhibitors

Inhibitor	Structure	Name and Molecular formula
(A)	 <p>The diagram shows a repeating unit of a cellulose derivative in its chair conformation, enclosed in large parentheses with a subscript 'n'. The glycosidic bond is shown as a dashed line extending from the oxygen atom at the C4 position to the left. The hydroxyl groups at the C2 and C6 positions are substituted with 'OR' groups. The 'OR' group at C2 is in the axial position, and the 'OR' group at C6 is in the equatorial position.</p>	Carboxy methyl cellulose $R = \text{CH}_2\text{CO}_2\text{H}$
(B)	 <p>The diagram shows a repeating unit of a cellulose derivative in its chair conformation, enclosed in large parentheses with a subscript 'n'. The glycosidic bond is shown as a dashed line extending from the oxygen atom at the C4 position to the left. The hydroxyl groups at the C2 and C6 positions are substituted with 'OR' groups. The 'OR' group at C2 is in the axial position, and the 'OR' group at C6 is in the equatorial position.</p>	Hydroxyl propyl cellulose $R = \text{CH}_2\text{CH}(\text{OH})\text{CH}_3$
(C)	 <p>The diagram shows a repeating unit of a cellulose derivative in its chair conformation, enclosed in large parentheses with a subscript 'n'. The glycosidic bond is shown as a dashed line extending from the oxygen atom at the C4 position to the left. The hydroxyl groups at the C2 and C6 positions are substituted with 'OR' groups. The 'OR' group at C2 is in the axial position, and the 'OR' group at C6 is in the equatorial position.</p>	Hydroxyl ethyl cellulose $R = \text{CH}_2\text{CH}_2\text{OH}$

3. RESULTS AND DISCUSSION

3.1- Weight loss measurements

The weight loss of carbon steel type 1018 specimen in 0.5 M HCl solution with and without different concentrations from the investigated inhibitors was determined after 3 h of immersion at 30 °C. Fig.1 represents this for compound (A) as an example. Similar curves were obtained for other inhibitors (not shown). The presence of inhibitors was found to reduce the corrosion rate.

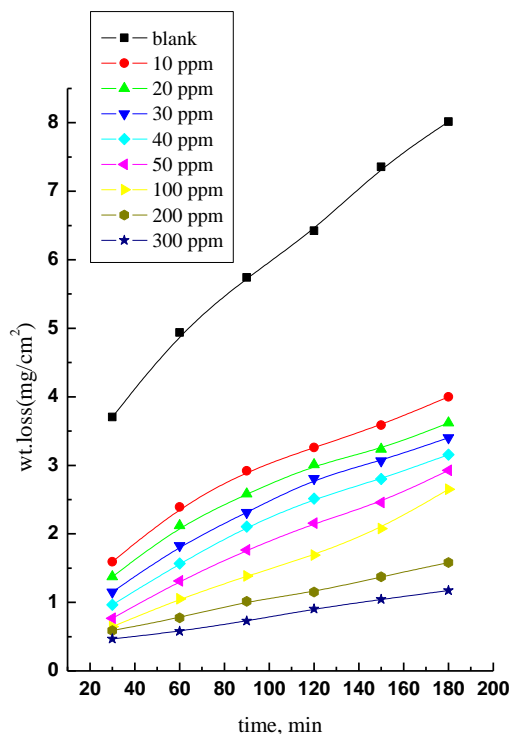


Fig. (1): Weight loss- time curves for the corrosion of carbon steel type 1018 in 0.5 M HCl in absence and presence of different concentrations of inhibitor (A) at 30 °C.

3.1.1- Adsorption isotherm

One of the most convenient ways of expressing adsorption quantitatively is by deriving the adsorption isotherm that characterizes the metal/inhibitor/environment system (Szkłarska-Smiałowska, 1991) various adsorption isotherms were applied to fit θ values which calculated from weight loss method but the best was found to obey Langmuir adsorption isotherm (Langmuir, 1947) which may be explained by:

$$(C/\theta) = 1/K + C \quad (5)$$

Where C is inhibitor concentration and K is equilibrium constant of adsorption see (Fig.2).

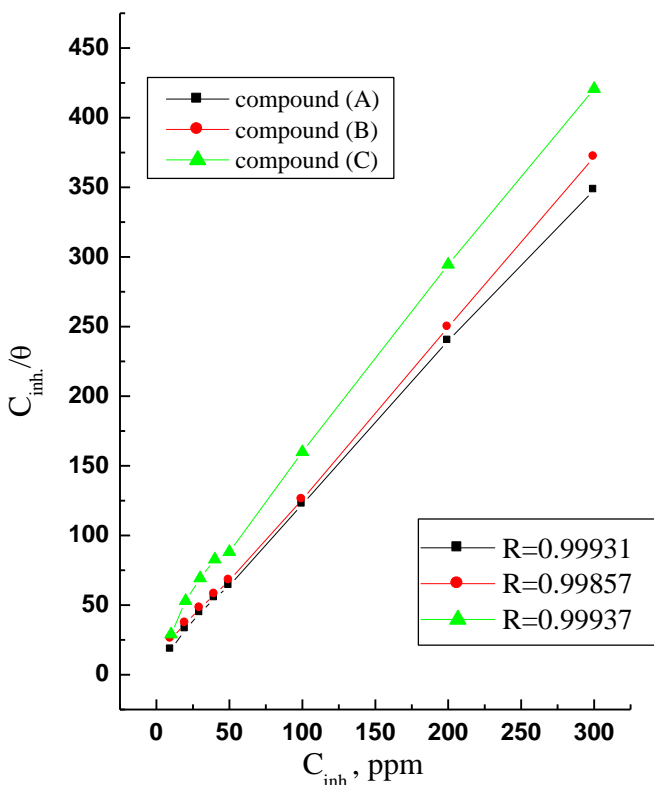


Fig. (2): Langmuir adsorption isotherm plotted as (C/θ) vs C of all inhibitors for corrosion of carbon steel type 1018 in 0.5 M HCl at 30 °C.

It is well known that the standard adsorption free energy ($\Delta G^{\circ}_{\text{ads}}$) is related to equilibrium constant of adsorption (K) and $\Delta G^{\circ}_{\text{ads}}$ can be calculated by the following equation (Khamis , 1990).

$$K = 1/55.5 \exp (- \Delta G^{\circ}_{\text{ads}}/RT) \quad (6)$$

Figure 2 represents the plot of (C/θ) against C for all investigated compounds. As can be seen from this figure, the Langmuir isotherm is the best one which explains the experimental results. Also, it is found that the kinetic-thermodynamic model of El-Awady et al (El-Awady & Ahmed , 1985) is valid to operate the present adsorption data.

$$\log (\theta / 1 - \theta) = \log K' - y \log C \quad (7)$$

$K = K'^{(1/y)}$, K' is constant and 1/y is the number of the surface active sites occupied by one inhibitor molecule. Plotting $\log (\theta / 1 - \theta)$ against $\log C$ for the compounds is given in Fig.3. where straight-line relationships were obtained suggesting the validity of this model for the studied case. The values of K and $\Delta G^{\circ}_{\text{ads}}$ calculated by Langmuir isotherm and 1/y, K and $\Delta G^{\circ}_{\text{ads}}$ calculated by the kinetic model are given in Table 2. The negative values of $\Delta G^{\circ}_{\text{ads}}$ suggested that the adsorption of inhibitor molecules onto steel surface is a spontaneous process. The magnitude of heat of adsorption reaches the magnitude of chemical reaction heat, which is the result of the transference of electron from donating atoms in the inhibitor molecule to the d-orbital of the iron atom. It is noting that the value of 1/y is more than unity. This means that the given inhibitor molecules will form monolayer on the steel surface. In general the values of $\Delta G^{\circ}_{\text{ads}}$ obtained from El-Awady et al model are comparable with those obtained from Langmuir isotherms.

Table (2): Inhibitor binding constants (K), free energy of binding ΔG_{ads}° , and number of active sites (1/y) for polymeric compounds at 300 ppm on carbon steel type 1018 surface in 0.5 M HCl at 30 °C

Inhibitors	Kinetic Model			Langmuir	
	1/y	K	$-\Delta G_{ads,1}^{\circ}, \text{kJ mol}^{-1}$	K	$-\Delta G_{ads,2}^{\circ}, \text{kJ mol}^{-1}$
Carboxy methyl cellulose	1.69	0.06	3.21	0.07	3.53
Hydroxy propyl cellulose	1.49	0.04	2.25	0.05	2.62
Hydroxy ethyl cellulose	2.64	0.01	1.14	0.04	1.8

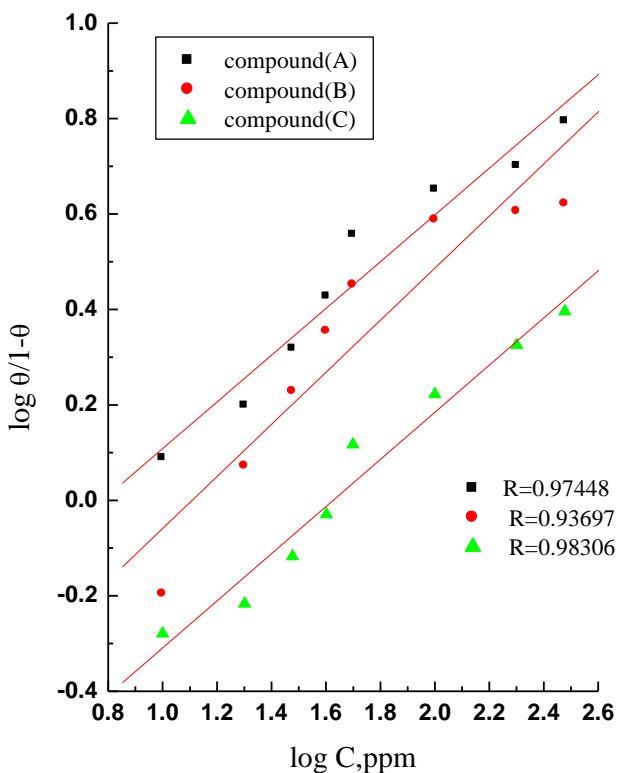


Fig. (3): El-Awady et al model plotted as $\log (\theta / 1 - \theta)$ vs $\log C$ of inhibitors for corrosion of carbon steel type 1018 in 0.5 M HCl solution at 30°C.

3.1.2- Kinetic parameters

The corrosion of carbon steel type 1018 in 0.5 M HCl in the absence and presence of different concentrations of the investigated inhibitors at temperatures ranges (30 – 60 °C) was studied using weight loss method. The percentage inhibition efficiency (η %) at each inhibitor concentration can be calculated using equation (2). The inhibition efficiency values at different temperatures for compound (A) was shown in Fig.4 and similar plots were obtained for the two inhibitors (not shown). The obtained data reveal that the extent of the inhibition efficiency increases with the concentration of the inhibitors and decreases with increasing temperature. These types of inhibitors retard the corrosion process at ordinary temperature (**Putilova et al., 1960**) whereas the inhibition is considerably decreased at elevated temperature. The increasing of the corrosion rate with increase the temperature is suggesting of physical adsorption of the investigated inhibitors on carbon steel type 1018 surface.

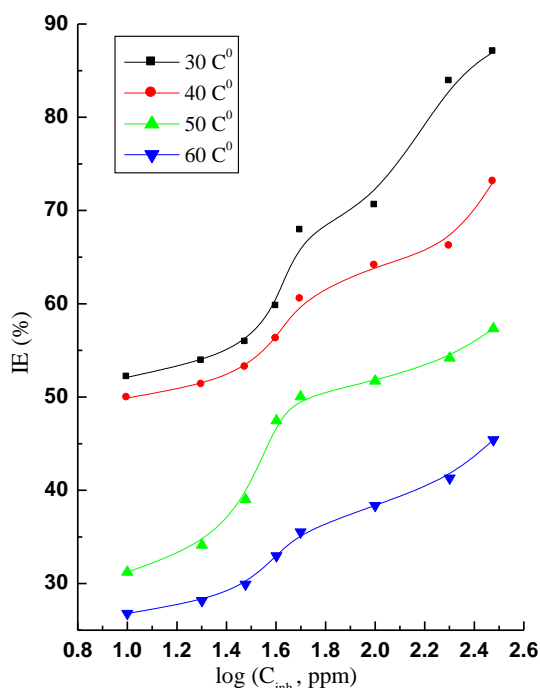


Fig. (4): Relationship between inhibition efficiency (η %) and concentration of compound (A) in 0.5 M HCl.

The activation energy of the corrosion process can be calculated using Arrhenius-type equation:

$$k = A \exp (-E_a^*/RT) \quad (8)$$

Where k is the corrosion rate, A is the pre-exponential factor, E_a^* is the apparent activation energy. R is the universal gas constant and T is the absolute temperature. The apparent activation energy at 300 ppm from the investigated inhibitors was calculated by linear regression between $\log k$ and $(1/T)$ Fig.5. The energy of activation for the investigated compounds and the values of the thermodynamic parameter for the dissolution of carbon steel type 1018 in 0.5 M HCl are listed in Table 3.

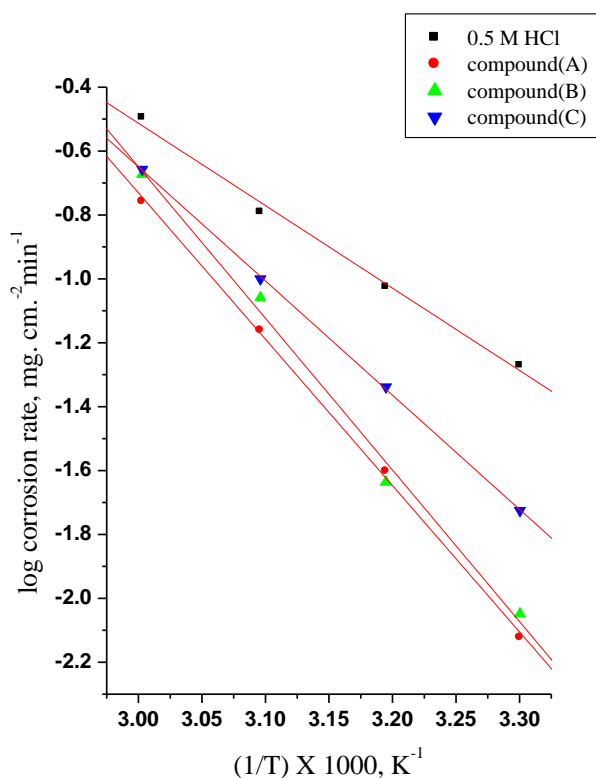


Fig. (5): Arrhenius plots ($\log k$ vs $1/T$) for carbon steel type 1018 in 0.5 M HCl in absence and presence of 300 ppm of inhibitors A, B and C.

$$R_{\text{corr}} = RT/Nh \exp (\Delta S^*/R) \exp (-\Delta H^*/RT) \quad (9)$$

Where h is Plank's constant and k is Boltzman's constant. The enthalpy of activation (ΔH^*) and the entropy of activation (ΔS^*) were calculated by applying the following equations (El-Awady & Ahmed, 1985).

$$\Delta H^* = E_a^* - RT \quad (10)$$

$$\Delta S^* = (\Delta H^* - \Delta G^*)/T \quad (11)$$

The activation energy is higher in the presence of additives than in their absence. The higher values of E_a^* are good evidence for the strong adsorption of polymeric compounds on the carbon steel surface. The values of (ΔH^*) are positive and high in the presence of the inhibitors over that of the uninhibited solution. This implies that energy barrier of the corrosion reaction in the presence of the investigated inhibitors increases. On the other hand ΔS^* values are lower and have negative values in presence of the inhibitors, this means that addition of these polymeric compounds cause a decrease in the disordering in going from reactants to the activated complexes (Gomma & Wahdan, 1995).

Table (3): Activation energy and thermodynamic activation parameters for dissolution of carbon steel type 1018 in 0.5 M HCl in absence and presence of 300 ppm of inhibitors at 30 °C

Inhibitors	E_a^* (kJ mol ⁻¹)	ΔH^* (kJ mol ⁻¹)	$-\Delta S^*$ (J mol ⁻¹ K ⁻¹)
0.5 M HCl	49.42	46.76	115.3
A	87.72	85.04	4.64
B	90.88	88.19	6.39
C	68.45	65.77	60.88

3.2. Polarization curves

Figure 6 illustrates the polarization curves of carbon steel in 0.5 M HCl solutions containing different concentrations of compound (A) at 30°C. The presence of compound (A) shifts both anodic and cathodic branches to the lower values of corrosion current densities and thus causes a remarkable decrease in the corrosion rate. The parameters derived from the polarization curves in Figure 6 are given in Table 4. Apparently, i_{corr} decreases considerably in the presence of compound (A).

The inhibition efficiency increases with increasing the compound (A) concentration. The Tafel slopes of β_c and β_a at 30°C do not change remarkably upon addition of compound (A), which indicates that the presence of compound (A) does not change the mechanism of hydrogen evolution and the metal dissolution process. Generally, an inhibitor can be classified as cathodic or anodic type if the shift of corrosion potential in the presence of the inhibitor is more than 85 mV with respect to that in the absence of the inhibitor (Tao et al., 2009; Satapathy et al., 2009; Ferreira et al., 2004; Yan et al., 2008; Li et al., 2008 and Riggs OL, 1973). These polymers could be classified as mixed-type inhibitors.

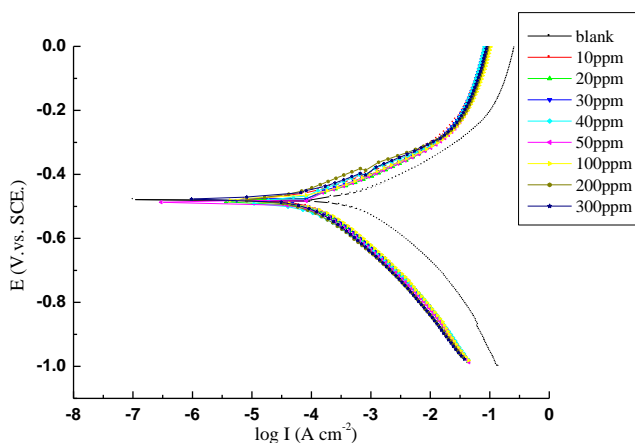


Fig. (6): Potentiodynamic polarization curves for carbon steel type 1018 in 0.5 M HCl in absence and presence of different concentrations of compound (A) at 30 °C.

Table (4): Effect of concentration of the investigated compounds on the free corrosion potential (E_{corr}), corrosion current density (i_{corr}), Tafel slopes (β_a, β_c), inhibition efficiency (% η), degree of surface coverage (θ) and corrosion rate for the corrosion of carbon steel type 1018 in 0.5 M HCl.

Concentration, ppm		i_{corr} $\mu A \text{ cm}^{-2}$	$-E_{corr}$ mV vs SCE	β_a mV dec ⁻¹	β_c mV dec ⁻¹	CR mpy	θ	% η
0.5 M HCl		511.6	479.3	96.46	138.9	152.1	-----	-----
Compound A	10	155.0	476.0	117.8	187.1	71.86	0.697	69.70
	20	144.0	484.0	121.3	177.7	67.03	0.718	71.85
	30	134.0	479.0	112.7	171.4	62.23	0.738	73.81
	40	126.0	488.0	127.6	171.0	58.33	0.753	75.37
	50	120.0	487.0	116.8	173.3	55.62	0.765	76.54
	100	114.0	481.0	107.3	158.3	52.83	0.777	77.72
	200	95.90	478.0	119.7	174.0	44.49	0.812	81.25
	300	95.80	477.0	106.2	171.4	44.43	0.812	81.27
Compound B	10	209.0	484.0	111.0	165.4	97.16	0.591	59.15
	20	181.0	481.0	97.30	149.1	84.01	0.646	64.62
	30	157.0	489.0	99.50	157.5	72.90	0.693	69.31
	40	147.0	487.0	100.2	163.7	68.31	0.712	71.27
	50	127.0	487.0	93.20	156.0	58.73	0.751	75.18
	100	118.0	485.0	88.80	153.1	54.84	0.769	76.94
	200	110.0	487.0	96.00	154.9	50.85	0.784	78.49
	300	101.0	485.0	88.50	145.9	46.87	0.802	80.26
Compound C	10	195.0	481.0	102.6	157.7	90.53	0.618	61.88
	20	193.0	480.0	104.8	159.2	89.43	0.622	62.28
	30	179.0	483.0	104.0	157.5	83.10	0.650	65.01
	40	173.0	482.0	100.6	156.6	80.13	0.661	66.18
	50	161.0	481.0	98.20	155.7	74.87	0.685	68.53
	100	145.0	480.0	95.80	139.7	67.21	0.716	71.66
	200	126.0	486.0	99.50	161.0	58.44	0.753	75.37
	300	114.0	480.0	94.10	138.8	52.79	0.777	77.72

3.3. Electrochemical impedance measurements (EIS)

Figures 7 and 8 show the Nyquist and Bode diagrams of carbon steel in 0.5 M HCl solutions containing different concentrations of compound (A) at 30°C. All the impedance spectra exhibit one single depressed semicircle. The diameter of semicircle increases with the increase of compound (A) concentration. The semicircular appearance shows that the corrosion of carbon steel is controlled by the charge transfer and the presence of compound (A) does not change the mechanism of carbon steel dissolution (Larabi et al., 2004). In addition, these Nyquist diagrams are not perfect semicircles. The deviation of semicircles from perfect circular shape is often referred to the frequency dispersion of interfacial impedance (Larabi et al., 2004 and Mansfeld et al., 1982). This behavior is usually attributed to the inhomogeneity of the metal surface arising from surface roughness or interfacial phenomena (Shih & Mansfeld 1989 and Martinez & Metikoš-Hukovic 2003), which is typical for solid metal electrodes (Bentiss et al., 2009). Generally, when a non-ideal frequency response is present, it is commonly accepted to employ the distributed circuit elements in the equivalent circuits. What most widely used is the constant phase element (CPE), which has a non-integer power dependence on the frequency (Trinstancho-Reyes et al., 2011 and Kissi et al., 2006). Thus, the equivalent circuit depicted in Figure 9 is employed to analyze the impedance spectra, where R_s represents the solution resistance, R_{ct} denotes the charge-transfer resistance, and a CPE instead of a pure capacitor represents the interfacial capacitance. The impedance of a CPE is described by the equation 12:

$$Z_{CPE} = Y^{-1} (j\omega)^{-n} \quad (12)$$

where Y_0 is the magnitude of the CPE, j is an imaginary number, ω is the angular frequency at which the imaginary component of the impedance reaches its maximum values and n is the deviation parameter of the CPE: $-1 \leq n \leq 1$. The values of the interfacial capacitance C_{dl} can be calculated from CPE parameter values Y_0 and n using equation 14 (Hsu & Mansfeld 2001):

$$C_{dl} = Y (\omega_{max})^{n-1} \quad (13)$$

The values of the parameters such as R_s , R_{ct} , Y_0 , n through EIS fitting as well as the derived parameters C_{dl} and η % are listed in Table 5.

As it is seen from Table 5, at 30°C the C_{dl} values decrease with the increase of compound (A) concentration, which suggests that STE functions by adsorption on the carbon steel surface. It is inferred that the compound (A) molecules gradually replace the water molecules by adsorption at the metal/solution interface, which leads to the formation of a protective film on the carbon steel surface and thus decreases the extent of the dissolution reaction (Bentiss et al., 2000). Moreover, the increase of compound (A) concentration leads to the increase of R_{ct} and η % values. The η % obtained from EIS measurements are close to those deduced from polarization method.

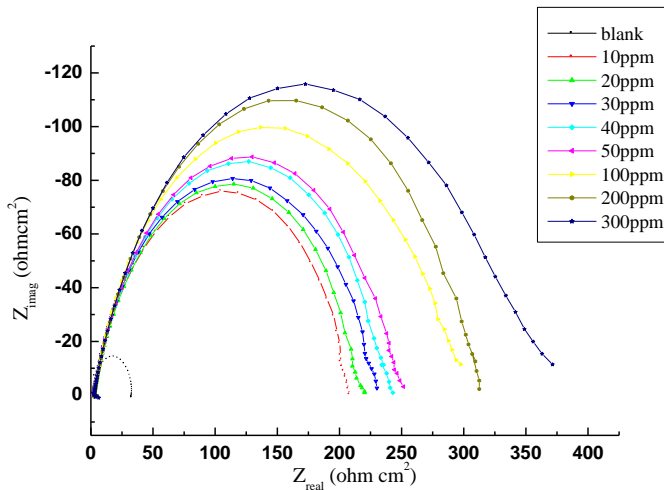


Fig.(7): Nyquist plots recorded for carbon steel type 1018 in 0.5 M HCl solutions without and with various concentrations of compound (A) at 30 °C.

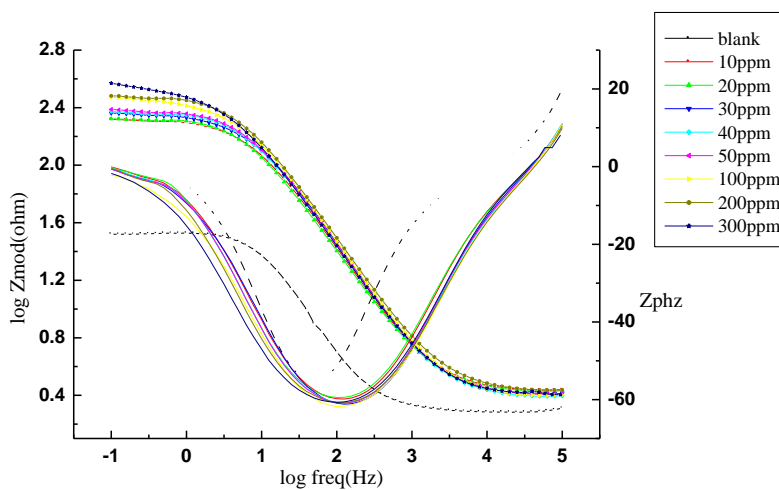


Fig. (8): Bode plots recorded for carbon steel type 1018 in 0.5 M HCl solutions without and with various concentrations of compound (A) at 30 °C.

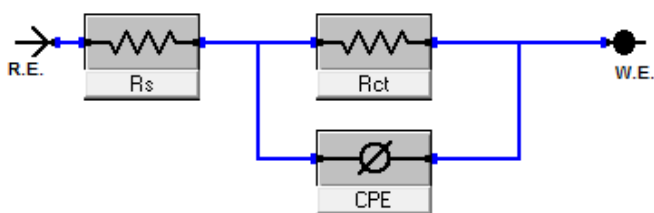


Fig. (9): Electrical equivalent circuit used to fit the impedance data.

Table (5): Electrochemical kinetic parameters obtained by EIS technique for carbon steel type 1018 in 0.5 M HCl solutions containing various concentrations of the investigated compounds at 30°C.

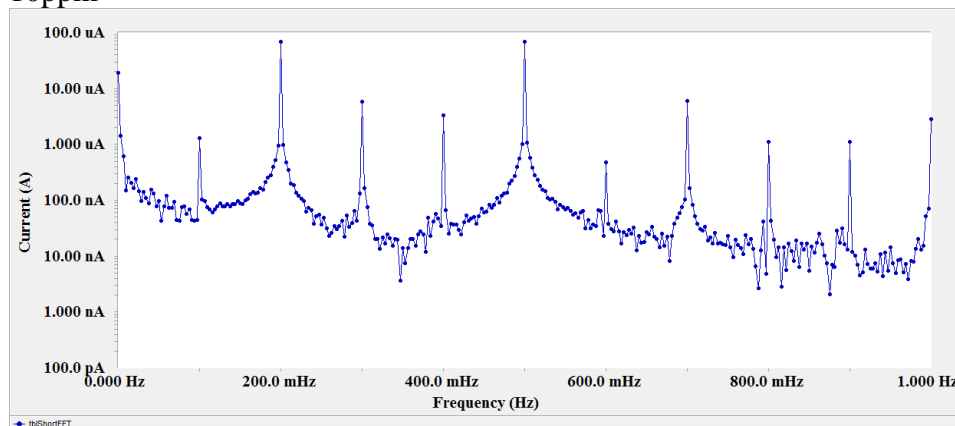
Concentration, ppm		R_{ct} , ohm cm^2	C_{dl} , $\mu F cm^{-2}$	θ	% η
0.5 M HCl		30.50	292.648	-----	-----
Compound A	10	206.4	105.827	0.852	85.2
	20	212.0	103.46	0.856	85.6
	30	225.0	102.869	0.864	86.4
	40	235.0	96.427	0.870	87.0
	50	240.9	94.618	0.873	87.3
	100	287.0	93.632	0.894	89.4
	200	303.9	92.313	0.899	89.9
	300	342.8	86.639	0.911	91.1
Compound B	10	162.0	148.293	0.812	81.2
	20	172.4	127.127	0.823	82.3
	30	178.4	126.423	0.829	82.9
	40	187.3	122.354	0.837	83.7
	50	190.0	120.383	0.840	84.0
	100	202.5	107.963	0.849	84.9
	200	207.1	84.402	0.853	85.3
	300	223.2	81.013	0.863	86.3
Compound C	10	162.2	182.636	0.812	81.2
	20	168.9	168.285	0.819	81.9
	30	174.9	162.504	0.826	82.6
	40	178.0	157.805	0.829	82.9
	50	184.6	154.815	0.835	83.5
	100	187.3	124.673	0.837	83.7
	200	190.7	122.436	0.840	84.0
	300	198.8	117.417	0.847	84.7

3.4. Electrochemical frequency modulation measurements (EFM)

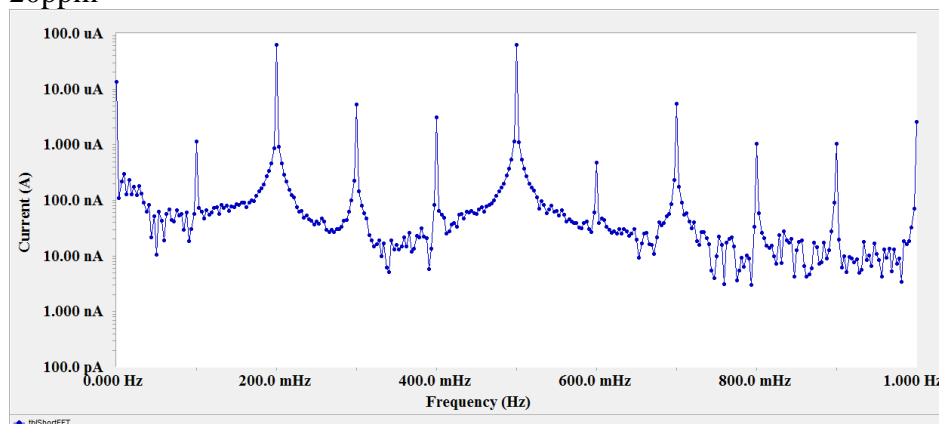
The EFM is a non destructive corrosion measurement technique that can directly give values of the corrosion current without prior knowledge of Tafel constants. Like EIS, it is a small ac signal. Intermodulation spectra obtained from EFM measurements of carbon steel in 0.5 M HCl solution in the absence and presence of different concentrations of the investigated polymer presented in Figure 10a-h. Each spectrum is a current response as a function of frequency.

The calculated corrosion kinetic parameters at different concentrations of the compound (A) in 0.5 M HCl at 30°C (i_{corr} , β_a , β_c , CF-2, CF-3 and $\eta\%$) are given in Table 6. From this Table, the corrosion current densities decrease by increasing the concentration of investigated polymer and the inhibition efficiencies increase by increasing investigated polymer concentrations. The causality factors in Table 6 are very close to theoretical values which according to EFM theory (**Bentiss et al., 2007**) should guarantee the validity of Tafel slopes and corrosion current densities. Values of causality factors in Table 6 indicate that the measured data are of good quality. The standard values for CF-2 and CF-3 are 2.0 and 3.0, respectively. The deviation of causality factors from their ideal values might due to that the perturbation amplitude was too small or that the resolution of the frequency spectrum is not high enough also another possible explanation that the inhibitor is not performing very well. The results showed good agreement of corrosion kinetic parameters obtained from EFM with the obtained from Tafel extrapolation and EIS methods.

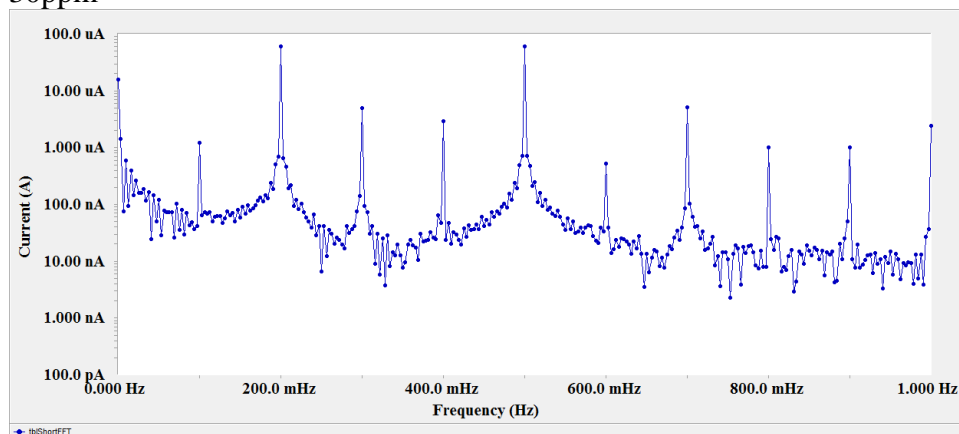
10ppm



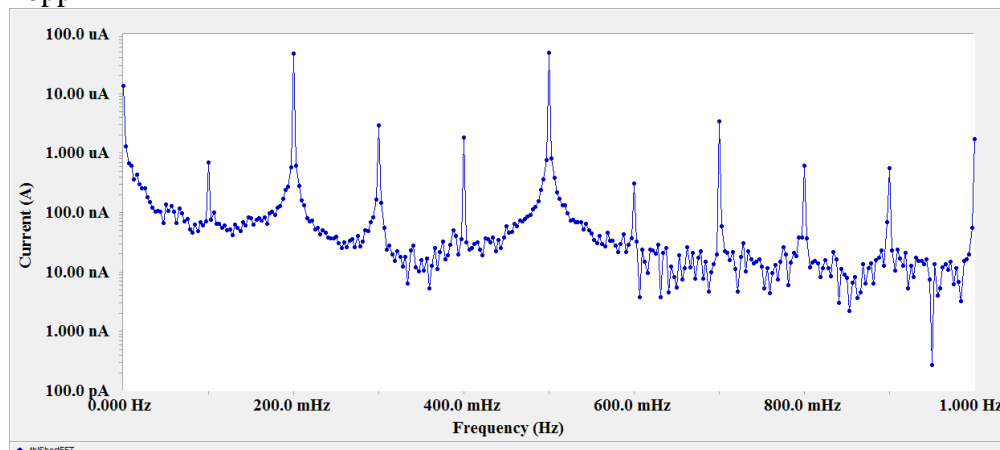
20ppm



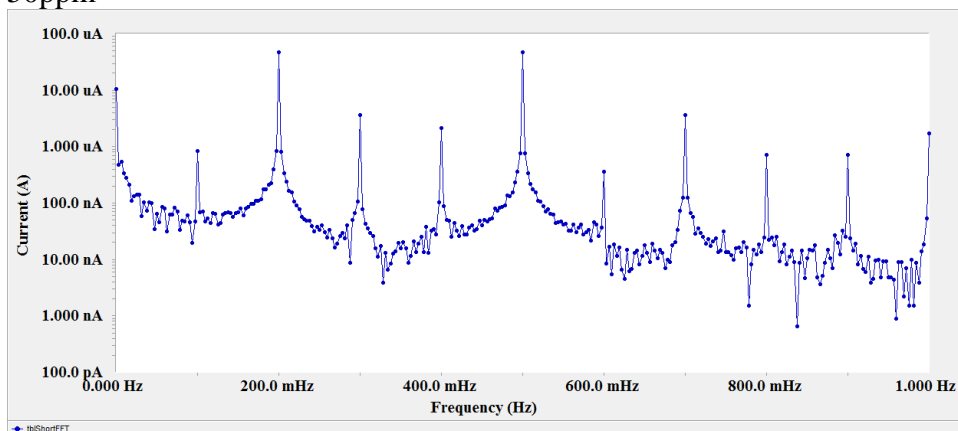
30ppm



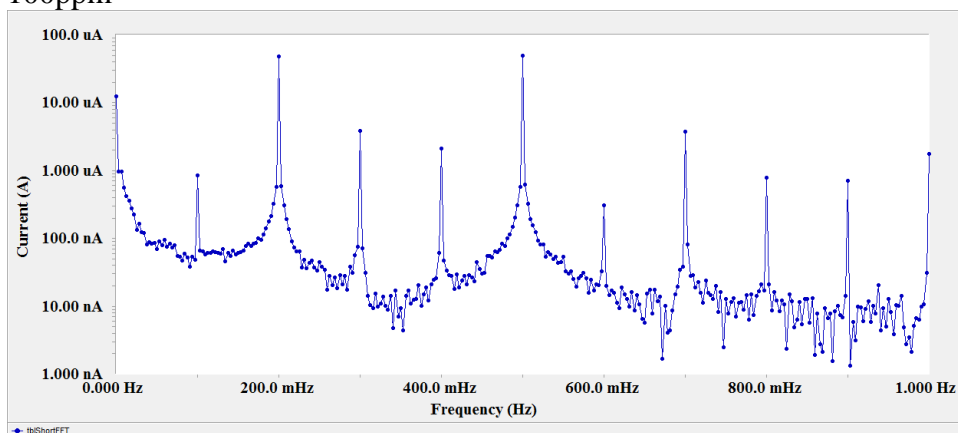
40ppm



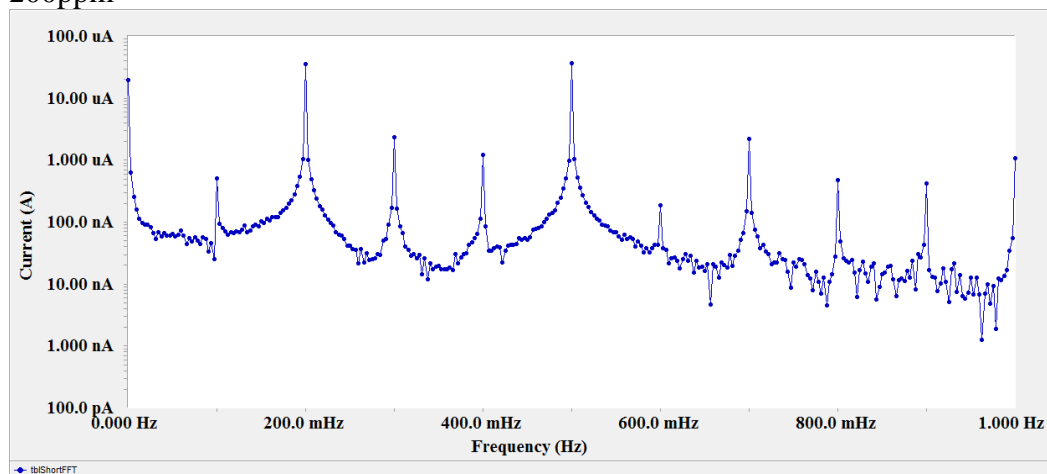
50ppm



100ppm



200ppm



300ppm

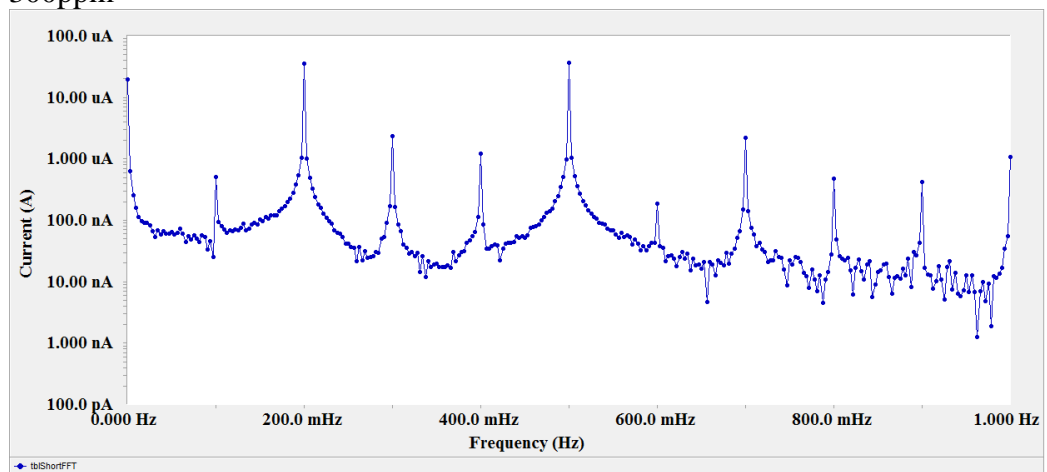


Fig. (10): Intermodulation spectra for C-steel in 0.5 M HCl in presence of different concentrations of compound (A).

Table (6): Electrochemical kinetic parameters obtained by EFM technique for carbon steel in 0.5 M HCl solutions containing various concentrations of the investigated compounds at 30°C.

3.5. Mechanism of inhibition

Many organic compounds with at least one polar unit containing atoms of nitrogen, sulfur and oxygen are known to function as corrosion inhibitors. The polar unit is regarded as the reaction centre for the adsorption process (**Anand et al., (1965)**). In such a case the adsorption bond strength is determined by the electron density on the atom acting as the reaction center and by polarisability of the unit. The polymeric compounds acting as corrosion inhibitors are adsorbed on the surface of the metal, forming a charge transfer complex between their polar atoms and the metal. It is apparent from the molecular structure that, these compounds can be adsorbed on the carbon steel surface through the lone pair of electrons of oxygen and delocalized π -electrons of benzene ring. The difference in the inhibition efficiencies can be explained on the number of oxygen atom in the cavity of these compounds.

The mode of adsorption (physiosorption and chemisorption) observed could be attributed to the fact that polymeric compounds contain many active centres, which some can adsorbed anodically and others adsorbed cathodically. This observation may be attributed to the fact that adsorbed organic molecules can influence the behaviour of electrochemical reactions involved in corrosion processes in several ways. The action of organic inhibitors depends on the type of interactions between the substance and the metallic surface. The interactions can bring about a change either in electrochemical mechanism or in the surface available for the processes (**Aramaki & Hackerman (1969)**); (**Singh & Quraishi (2010)**).

The order of inhibition efficiency of these polymeric compounds is as follows: (A) > (B) > (C) This is attributed to the presence of large number of O-atoms in these molecules. These molecules cover a large area of carbon steel. Compound (A) contains carbonyl group, compound (B) contains OH-group but branched and compound (C) contains OH-group but not branched.

4. CONCLUSIONS

1. The investigated polymeric compounds are good inhibitors and act as mixed type inhibitors for carbon steel corrosion in HCl solution.
2. The results obtained from all electrochemical measurements show that the inhibiting properties increase with inhibitor concentration. The % η is in accordance to the order: $A > B > C$ with small differences in their numerical values.
3. Double layer capacitances decrease with respect to blank solution when the polymeric compounds added. This fact may explain by adsorption of polymeric compounds molecules on the carbon steel surface.
4. The adsorption of polymeric compounds on carbon steel surface in HCl solution follows Langmuir adsorption isotherm.
5. The negative values of $\Delta G^{\circ}_{\text{ads}}$ show the spontaneity of the adsorption.
6. The values of inhibition efficiencies obtained from the different independent quantitative techniques used showed the validity of the results.

5. REFERENCES

- Abdel-Rehim, S.S., Khaled, K.F., Abd-Elshafi, N.S., (2006). *Electrochim. Acta* 51, 3269.
- Anand, R.R., Hurd, R.M., Hackerman, N., (1965). *J. Electrochem. Soc.* 112, 138.
- Aramaki, K., Hackerman, N., (1969). *J. Electrochem. Soc.* 116, 568.
- Bentiss, F., Bouanis, M., Mernari, B., Traisnel, M., Vezin, H., Lagrenee, M., (2007). *Appl. Surf. Sci.* 253, 3696.
- Bentiss, F., Lebrini, M., Vezin, H., Chai, F., Traisnel, M., Lagrené, M., (2009). *Corros. Sci.* 51, 2165.
- Bentiss, F., Traisnel, M., Lagrenee, M., (2000). *Corros. Sci.* 42, 127.
- Bosch, R.W., Hubrecht, J., Bogaerts, W.F., Syrett, B.C., (2001). *Corrosion* 57, 60.

da Rocha, J.C., Gomes, J.A.C.P., D'Elia, E., (2010). *Corros. Sci.* 52, 2341.

El-Awady, A. Y. and Ahmed, I. A., (1985). *Ind. J. Chem.*, 24A, 601.

Ferreira, E.S., Giacomelli, C., Giacomelli, F.C., Spinelli, A., (2004). *Mater. Chem. Phys.* 83, 129.

Gomma, K. M. and Wahdan, H. M., (1995). *Mater. Chem. Phys.*, 39, 209.

Hsu, C.S., Mansfeld, F., (2001). *Corrosion* 57, 747.

Kissi, M., Bouklah, M., Hammouti, B., Benkaddour, M., (2006) *Appl. Surf. Sci.* 252, 4190.

Langmuir, A. I., (1947). *J. Chem. Soc.*, 39, 1848.

Larabi, L., Harek, Y., Traianel, M., Mansri, A., (2004). *J. Appl. Electrochem.* 34, 833.

Lehr, I. L. and Saidman, S. B., (2006). *Electrochim. Acta*, 51, 3249–3255.

Li, W.H., He, Q., Zhang, S.T., Pei, C.L., Hou, B.R., (2008) *J. Appl. Electrochem.* 38, 289.

Mansfeld, F., Kendig, M.W., Tsai, S., (1982). *Corrosion* 38, 570.

Martinez, S., Metikoš-Hukovic, M., (2003). *J. Appl. Electrochem.* 33, 1137.

Parikh, K.S., Joshi, K.J., (2004). *Trans. SAEST.* 39, 29.

Parr, R.G., Donnelly, R.A., Levy, M., Palke, W.E., (1978). *J. Chem. Phys.* 68, 3801.

Putilova, K. I., Balizen, A. S. and Barasanik, P. Y., (1960). *Metallic corrosion inhibitors*, Pergamon Press. Oxford, P.30.

Rajendran, S., Sridevi, S. P., Anthony, N., Amalraj, A. J. and Sundaravadivedi, M., (2005). *Anti-corros. Methods Mater.*, 52, 102.

Riggs, O.L., Jr. (1973) *Corrosion Inhibitors*. 2nd Ed. NACE, Houston, TX, p. 11.

Satapathy, A.K., Gunasekaran, G., Sahoo, S.C., Amit, K., Rodrigues, R.V., (2009). *Corros. Sci.* 51, 2848.

Shih, H., Mansfeld, F., (1989). *Corros. Sci.* 29, 1235.

Singh, A.K., Quraishi, M.A., 2010. *Corros. Sci.* 52, (1529).

Solomon, M. M., Umoren, S. A., Udosoro, I. I., Udoh, A. P., (2010). *Corros. Sci.* 52, 1317

Szklarska-Smiałowska, Z., (1991). *Electrochemical and Optical Techniques for the study of Metallic Corrosion*, Kluwer Academic, the Netherlands; 545.

Tao, Z.H., Zhang, S.T., Li, W.H., Hou, B.R., (2009). *Corros. Sci.* 51, 2588.

Torres, V.V., Amado, R.S., Faia de Sá, C., Fernandez, T.L., Riehl, C.A.S., Torres, A.G., D'Elia, E., (2011). *Corros. Sci.* 53, 2385.

Trinstancho-Reyes, J.L., Sanchez-Carrillo, M., Sandoval-Jabalera, R., Orozco-Carmona, V.M., Almeraya-Calderon, F., Chacon-Nava, J.G., Gonzalez-Rodriguez, J.G., Martínez-Villafane, A., (2011). *Int. J. Electrochem. Sci.* 6, 419.

Yan, Y., Li, W.H., Cai, L.K., Hou, B.R., (2008). *Electrochim. Acta* 53, 5953.

امتزاز و تثبيط تآكل بعض المركبات البوليمرية على الصلب الكربون في المحاليل الحمضية

عبدالفتاح محمد عوف - أميره محمد عبد الحفيظ - هانم عبدالرسول مصطفى

قسم الكيمياء - كلية العلوم - جامعة المنصورة

التآكل هو المشكلة الرئيسية التي تهدد فترة عمر صلاحية المعدن للاستخدام وفهم ميكانيكية التآكل يمكننا من إيجاد حل مشاكل التآكل الحالية ومنع المشاكل المستقبلية وهذا البحث يناقش تآكل الصلب الكربوني في حامض الهيدروكلوريك وكيفية حمايته. تم دراسة تأثير المثبطات البوليمرية علي تآكل الصلب الكربوني في ٠,٥ مول حمض الهيدروكلوريك باستخدام الطرق التالية: (طريقة فقد الوزن والاستقطاب البتتشيوديناميكي و المعاوقة الكهربية و التردد الكهروكيميائي المعدل) وقد وجد أن كفاءة التثبيط تزداد بزيادة التركيز وتقل بزيادة درجة الحرارة وتم حساب بعض الدوال الترموديناميكية لعملية التثبيط والادمصاص وقد وجد أن هذه المركبات البوليمرية تعمل كمثبطات مختلطة وتدمص علي سطح الصلب الكربوني تابعة ايزوثرم لانجمير وقد وجد أن كفاءة تثبيط المركبات يعتمد علي الشكل الفراغي للمركبات والمراكز النشطة الموجودة في المركبات التي تحدد الكثافة الالكترونية علي سطح الصلب الكربوني ووجد أن النتائج المتحصل عليها من الطرق الأربعة متطابقة تماما.